PAPER 19 (SESSION II)

An experimental study of the critical tensile stress criterion for cleavage fracture in 3% silicon-iron

J. R. GRIFFITHS and G. OATES

Central Electricity Research Laboratories, Leatherhead, Surrey, England

Summary

The cleavage fracture stress and the fracture energy for coarse-grained 3% silicon iron have been derived from experimental results on notch-bend and uniaxial tension specimens. The macroscopic tensile stress (σ_F) beneath a notch at fracture was found in two different ways, one based on observations made when fracture coincided with general yield, and the other on observations made for fracture well below general yield. Differences in the results for the two techniques are accounted for and it is concluded that the general yield technique gave more reliable values. Measurements of the fracture energy for the notched and smooth specimens were derived from the appropriate fracture stress values together with the previously established sizes of the microcracks which initiated final fracture. These energy values were some 100 times less than those calculated by the methods of linear elastic fracture mechanics: the discrepancy is due to the plastic work involved in providing a mechanism for complete fracture.

Introduction

It was suggested by Orowan in 1948 [1] that cleavage fracture occurs at a critical tensile stress (σ_F) which is relatively independent of temperature and strain rate but dependent on the plastic strain preceding fracture. This hypothesis has been widely used to interpret cleavage fracture behaviour, in particular to explain notch effects, but it has proved difficult to examine the hypothesis critically by analysing the triaxial stress state induced by notches at fracture. Recent investigations of the yield and fracture behaviour of notched bars loaded in plane strain bending [2 - 5] have enabled estimates to be made of the maximum longitudinal stress when fracture occurs at various temperatures and strain rates. These investigations fall into two categories. One approach is to vary the degree of hydrostatic stress at fracture by varying the included notch angle. It has been shown from slip-line field theory [6] that for a notch-bend specimen of the type shown in Fig. 1 the maximum tensile stress (σ_{max}), at the plastic-elastic interface at general yield is given by the relationship:

$$\sigma_{max} = 2\tau_y\left(1 + \frac{\pi}{2} - \frac{\theta}{2}\right) \qquad (1)$$

where τ_y is the shear yield stress and θ the included notch angle in radians. The relation is valid for included angles > 6·4 °. Expressing equation

1 in terms of the uniaxial yield stress (σ_y) may be done assuming an appropriate yield criterion:

$$\text{(von Mises)} \quad \sigma_{max} = \frac{2\sqrt{3}}{3}\,\sigma_y\left(1 + \frac{\pi}{2} - \frac{\theta}{2}\right) \tag{2}$$

$$\text{(Tresca)} \quad \sigma_{max} = \sigma_y\left(1 + \frac{\pi}{2} - \frac{\theta}{2}\right) \tag{3}$$

Thus, by varying the notch angle, the maximum local stress at general yield can be altered and by determining the temperature, T_{GY}, at which fracture occurs at general yield for each notch angle, the maximum macroscopic tensile stress (σ_F) beneath the notch at fracture can be calculated.

The second approach is to test specimens under conditions giving fracture at loads well below the general yield load (L_{GY}). At such loads the plastic zone is confined to the vicinity of the notch root, the slip lines having the form of logarithmic spirals [2, 7, 8]. The longitudinal stress (σ_1) within the plastic zone is given by a relationship due to Hill [7]:

$$\sigma_1 = 2\tau_y\left[1 + \ln\left(1 + \frac{x}{r}\right)\right]; \; x \leqslant R \tag{4}$$

where x is the distance below the notch, r the notch root radius and R the plastic zone size (Fig. 2). At a given zone size, σ_1 reaches a maximum at the plastic-elastic interface where

$$\sigma_1 = 2\tau_y\left[1 + \ln\left(1 + \frac{R}{r}\right)\right] \tag{5}$$

and, as the plastic zone develops under increasing applied load, σ_1 at the interface increases. Eventually, a zone size R' is achieved at which σ_1 at the interface reaches σ_{max}, (equation 1) and then

$$\sigma_1 = 2\tau_y\left[1 + \ln\left(1 + \frac{R'}{r}\right)\right] = 2\tau_y\left(1 + \frac{\pi}{2} - \frac{\theta}{2}\right) \tag{6}$$

For zone sizes $> R'$, σ_1 remains constant [9] in the region $R' \leqslant x \leqslant R$ and has the value σ_{max} (Fig. 3).

If notch-bend specimens are tested under conditions giving cleavage failure at loads $<\sim 0{\cdot}6\, L_{GY}$, and if a method is available for assessing the plastic zone size at fracture, then the tensile stress (σ_F) at the plastic-elastic interface at fracture can be calculated using relation 5.

Results in support of the critical tensile stress criterion for cleavage fracture have been obtained for various mild steels using both the general yield technique [3 - 5] and the method based on Hill's relationship [2].

However, although the materials studied were fairly similar, the values of σ_F quoted differed widely, being typically ~ 135 kg/mm^2 using Hill's relationship and 80 - 90 kg/mm^2 for the general yield technique. In addition, Oates [4, 5] showed that the microstructural changes brought about by the addition to 1½% Mn to mild steel produce a substantial increase in σ_F (deduced by the general yield technique) and introduce a strong temperature and strain rate dependence. This last result, which shows that Orowan's criterion is not universally applicable, was explained in terms of the different operative mechanisms of cleavage fracture initiation in the high manganese steel under conditions giving fracture at general yield.

The main object of the present investigation was to compare critically the general yield and the method based on Hill's relationship, to establish the cause of the apparent incompatibility of earlier results. A brittle 3% silicon iron was chosen since this material fails by cleavage over a wide range of temperature and since plastically deformed regions may be detected by etch pitting methods. The operative mechanisms of cleavage fracture in these specimens were first established over the complete temperature range of interest and this work has been reported previously [10]. To establish these mechanisms was considered essential in view of the results found for high Mn steel and also since the respective temperature ranges over which the two techniques give valid results would inevitably differ.

Experimental method and results

The composition of the silicon iron is given in Table I.

The material was supplied as slabs, 3·2 cm thick, having a very coarse grain size (0·4 mm). The slabs were heated for 1 hour at 850 °C, hot-rolled to 2·5 cm thickness, air-cooled to $\sim$200 °C, rolled to 1·5 cm thickness at this temperature, and then air-cooled.

Hounsfield 'no. 13' tensile specimens, and 4 point notchbend specimens (Fig. 1) were prepared at this stage; all specimens were machined such that their length was along the rolling direction and the notches were cut parallel to the slab face. After machining, all specimens were sealed in evacuated silica capsules, heated for 3½ hours at 1100 °C and furnace cooled; this gave a ferrite grain size of 0·09 mm, measured by the linear intercept method. The structure was equiaxed ferrite grains with $\sim$0·5% of rather coarse lamellar pearlite surrounded by envelopes of cementite, and grain boundary films of cementite. These films were mainly $\sim$1 micron or less in thickness but there was a small percentage with thickness in the range 2 - 3 microns.

Both tensile and notch-bend tests were done on a 5-ton testing machine at a constant crosshead speed of 0·2 cm/min. Test temperatures were achieved by immersing specimens in various liquid or vapour baths, and were maintained throughout each test to within ± 1 deg. C. The notch angle was varied between 45° and 120° and the temperature, T_{GY}, at which fracture coincided with general yielding was found for each angle. Bars with 45° notches were tested between −196 and +60 °C, as were the tensile specimens. In addition to the specimens tested to failure, 45° notched bars were loaded to various fractions of general yield, unloaded, aged for 40 min at 170 °C and then etch pitted [11] to reveal the extent of plastic yielding below the notch.

The results of the mechanical tests on smooth and 45° notch-bend specimens are given in Fig. 4 and 5 respectively; the operative mechanisms of cleavage fracture, established earlier [10] are summarised briefly below. In uniaxial tension the critical fracture event between ~−50 °C and +55 °C (Region C) was the growth of grain size microcracks but below ~−50 °C (Regions A, B) fracture was nucleation controlled. In Region A (< −120 °C) fracture occurred below the macroscopic yield stress and was twin nucleated: between −120 °C and ~−50 °C (Region B) the twinning stress coincided with the slip yield stress and specimens fractured after a small amount of plastic strain. Above −50 °C only a few isolated twins were formed. In the notch-bend specimens the critical fracture event throughout the range −160 °C to +60 °C was growth of slip-induced carbide cracks; below −160 °C twinning was involved in the fracture process. The plastic zone size measurements in the notched bars are given in Fig. 6. Yielding was confined to the notch root region for loads up to about 0·6 L_{GY}: at 0·7 L_{GY} far-reaching 'wings' had begun to form which eventually traversed the cross-section at general yield.

Values of the maximum stress at fracture, σ_F, in the notched specimens were calculated (Fig. 7) using the two methods described in the Introduction and assuming the von Mises yield criterion. The temperature at which bars containing notches of various angles broke at general yield varied from −20 to +40 °C and so the general yield method could only be used between these limits. Regarding the other method, relation 5 is valid for zone sizes < R' where R' is found from relation 6 and, for the 45° notched specimens, is 0·56 mm. Since (Fig. 6) this zone size is attained at 0·6 L_{GY} the method can only be used when the fracture loads are less than this, i.e. below −65 °C. Additionally, calculations of σ_F were made for fractures at loads between 0·6 and 1·0 L_{GY} (−65 to +40 °C) assuming throughout the stress intensification given by relation 6. Fig. 7 also includes the fracture stresses for the uniaxial tensile specimens tested above −50 °C. Results for lower temperatures where fracture was nucleation controlled are not included since the measured quantity reflects a yield rather than a fracture stress.

The fracture stress, σ_F, and the size, c, of the internal crack which initiates final fracture are related to the effective fracture energy, γ, by the Griffith equation.

$$\sigma_F = \left[\frac{4E\gamma}{\pi c(1-\nu^2)}\right]^{1/2} \tag{7}$$

where E is Young's modulus and the stress state corresponds to plane strain. Thus, once c is known for the particular fracture mechanism, values for γ can be found. In the bend specimens the stress is not a uniform tension, but, since it varies slowly compared to the crack dimensions, the errors in γ will be small. When the size of microcrack is small compared to the length of the slip bands which nucleated it, the additional stresses on the crack due to the dislocations should be considered in addition to the direct stress [4, 5, 12]. However, although this situation did arise in the present work when fracture was nucleated from cracked carbides, the simple form (equation 7) has been used since the differences were not large. Values of γ are plotted in Fig. 8 for the plain tensile specimens fractured between ~−50 and +55 °C (c = 0·09 mm.) and for the notch-bend specimens fractured between −160 and + 40 °C (c = 0·002 mm.).

The notch-bend experiments done at less than ~−30 °C are, except for the blunt notch geometry, valid plane strain fracture mechanics tests. Values for the critical stress intensity factor, K_{Ic}, were found using the standard analysis [13]: values for G_{Ic} (=γ) were derived by putting $EG_{Ic} = K_{Ic}^2$ and varied from 8×10^6 ergs/cm² at −30°C, to 30×10^6 ergs/cm² at −196 °C. It has been shown [14] that the effect of fatigue cracking on the notched fracture strength of mild steel reduces by a factor of not more than four the value of G_c over a temperature range comparable to that covered in these experiments, and further work on silicon iron at −196 °C [15, 16] has confirmed this. The probable appropriate values for G_{Ic} are thus in the range 2×10^6 ergs/cm² to 1×10^6 ergs/cm² between −30 and −196 °C. These results are plotted in Fig. 8.

Discussion

General yield and pre-general yield methods for σ_F and γ

At temperatures between −160 and −65°C, where the plastic zone size at fracture was $\leqslant R'$, the σ_F values calculated using Hill's relationship are independent of temperature (Fig. 7). This supports the hypothesis proposed by Orowan and is in agreement with earlier work [2]. However, at temperatures below −160 °C, where fracture was probably associated with mechanical twinning, σ_F decreases with temperature. This may arise because of a transition to nucleation controlled fracture or, alternatively, may reflect the contribution to the fracture process of twinning dislocations involved in crack nucleation [4, 5]. Between −20 and +40 °C, σ_F calculated using the general yield method increased with temperature, as did the cleavage fracture strength of smooth specimens over the same temperature range. This evidence shows that the fracture criterion proposed by Orowan does not apply throughout the cleavage fracture region studied.

Clearly, the level of σ_F and γ found from equations (1 and 5) are widely different (Figs. 7 and 8) and as used here these equations appear to be incompatible. A similar conclusion has recently been reached [17] although no explanation was proposed. There are several factors which may contribute towards the observed differences. Firstly, statistical considerations [10, 18] lead to the prediction that σ_F will be higher when fracture occurs well before rather than at general yield due to the smaller volume of highly stressed material. Suppose the fracture criterion has the form [18].

$$\sigma^m V = \text{constant} \tag{8}$$

where V is the volume of material at the stress σ and m is of the order of twenty [19]. The volume of material within one grain diameter of the maximum tensile stress region at loads $<0{\cdot}6L_{GY}$ is $\sim d^2B$ where d is the grain diameter and B the specimen width. The volume of material under the maximum tensile stress at general yield (Fig. 3) is $\sim (R - R')\, dB\ mm^3$ which, assuming $R = 0{\cdot}98$ mm for the 45° notched specimens [9], is $\sim 0{\cdot}42dB mm^3$. Substituting in equation (8) gives $\sigma_F \sim 8\%$ higher for fracture at $< 0{;}6L_{GY}$ compared with σ_F for general yield; the difference in Fig. 7 is > 50%.

A further possibility is that work hardening will affect calculations based on a rigid–perfectly plastic model. Below $0{\cdot}6L_{GY}$ the notch root strains are <~1% and work hardening will be slight; at general yield the notch root strain is ~7% [20] and the local yield stress will have been raised by about 25%. However, even if this local hardening is fully reflected at the elastic-plastic interface the effect is still not sufficient to account for the observed discrepancy. Furthermore, the variation of σ_F with temperature (Fig. 7) found for 45° notched specimens fractured above −65°C is incompatible with an explanation in terms of work hardening. Even at $0{\cdot}8L_{GY}$ the notch root strain is only 2 to 2½% and so very small effects would be predicted below this load, i.e. below ~ −5°C. There is, however, a marked decrease in σ_F (calculated from equation 6) with increasing temperature in the range −65 to −5°C (Fig. 7).

It is concluded from the above discussion that work hardening and statistical effects cannot account for the observed differences in σ_F obtained by the two techniques. One way in which the two approaches can be reconciled is to assume that fracture is not nucleated at the elastic-plastic

interface, but at some distance behind it. This could come about if, as mechanistic studies suggest [10] a certain plastic strain, ϵ_F, is necessary to achieve a sufficient number of cracked carbides to give a reasonable chance of fracture. To test this hypothesis rigorously an analysis of strain as a function of stress and distance from the notch root is needed, together with a knowledge of the magnitude and the variation of ϵ_F with temperature and stress stage. Although approximate elastic solutions for the strain field may be found [21, 22] a detailed elastic-plastic analysis does not exist. However, it can be seen in a qualitative way [16] that the strain below the notch falls off steeply at first and then more gradually at the elastic-plastic interface. To achieve even a small plastic strain, therefore, it is necessary to go a relatively large distance back from the elastic-plastic interface with a consequent lowering of the effective stress intensification (equation 4). Approximate calculations indicate that between −30 and −160°C a critical strain of about 0·5% would be sufficient to reduce σ_F from the values derived from equations (5) and (6) to about 80 kg/mm². At general yield, however, a region of constant stress intensification is found at the tip of the plastic zone (Fig. 3): since it is possible to accommodate small plastic strains within this region the value of σ_F found from equation (1) is still appropriate. The decrease in σ_F with temperature for the 45° notched specimens above −65 °C (Fig. 7) is consistent with a critical strain hypothesis; as the plastic zone size increases beyond R' so does the distance over which σ_{max} is achieved and the closer the calculated σ_F approaches the value relevant to the fracture process. Since the calculations based on equation (5) are so sensitive to small values of ϵ_F we conclude that the general yield approach gives the more reliable estimate of fracture stress. Accordingly, self consistent values for σ_F and γ can be given for the range −160 °C to +40 °C (Figs. 7, 8).

Comparison between notched and un-notched specimens

The way in which a deep notch can cause cleavage fracture in a material which exhibits fibrous fracture in uniaxial tension is well known and, under such circumstances, comparison of the two fracture stresses is not meaningful. When, however, both notched and un-notched specimens fail by cleavage it might be hoped that a direct comparison might be made. Metallographic observations [10] show, however, that no such comparison can be made for this material at any temperature. This is because for the tensile tests there was only one region (~−50 °C to + 57 °C, Fig. 4) where it was possible to measure γ for crack propagation and this was associated with the growth of a grain size microcrack; for the notched tests values were found from −160 °C to +40 °C but these were associated with the growth of carbide size microcracks. A difference in the two values of γ

is thus to be expected. Irrespective of the different fracture mechanisms, it is clear from Fig. 4 that carbide cracks in plain specimens propagate into the ferrite at lower stresses than those deduced for notched specimens at general yield. It is suggested that these differences are largely associated with statistical effects as discussed earlier.

Implications for fracture mechanics

Although it has been possible, in the preceding paragraph, to suggest a way in which equations (1) and (5) can be used to give consistent results it remains that the fracture energy found by these methods is 100 times smaller than G_{Ic} found by fracture mechanics principles. This may be understood by considering the physical significance of the various measurements. The critical stage in the fracture process is the growth of a suitable carbide crack into ferrite or pearlite and the low γ found from the microscopic approach corresponds to the effective fracture energy for such growth. However, to propagate the carbide crack requires a tensile stress σ_F and to achieve this stress a sufficient stress intensification must be developed. The high γ found from fracture mechanics corresponds to the work done in growing the necessary plastic zone.

The magnitude of G_{Ic} will depend upon the mechanism of producing a dynamic crack ahead of the main crack or notch; it is not, as commonly held, simply the energy required from thermodynamic considerations to extend the main crack unit amount. This interpretation is, of course, similar to previous suggestions [23, 24] that G_{Ic} can be estimated from the product of the yield stress and the notch tip displacement. Calculations using this method give broadly similar results to those obtained using linear elastic fracture mechanics.

Conclusions

Measurements of the cleavage fracture stress, σ_F, have been made in notched bars using two different techniques which involved fracturing the specimens either at, or well below, general yield. The two methods gave widely different values for σ_F which cannot be explained in terms of work hardening and statistical effects. However, the differences can be accounted for by assuming that the cleavage mechanism requires a small plastic strain for its operation. At higher temperatures (40 °C to $\sim$−20 °C) σ_F varied with temperature but below $\sim$−20 °C became approximately temperature independent. The values of σ_F from the notched specimens were compared to those of plain tensile specimens, and, although the temperature dependence found at higher temperatures was repeated, the absolute values were lower for the tensile specimens.

Values for the fracture energy, γ, were calculated for smooth and notched

specimens using the measured σ_F and taking account of the sizes of the microcracks present in the specimens at fracture. Differences between the two types of specimen were due to the different operative fracture mechanisms. Estimates of the fracture energy were also made from linear elastic fracture mechanics and were $\sim$100 times larger than the values derived from microstructural considerations. It is suggested that this factor arises from the difficulty of nucleating fracture under a notch which meant that a significant plastic zone had to be formed, absorbing a large amount of energy.

References

1. OROWAN, E. 'Fracture and strength of solids'. *Reports of Progress in Physics*, vol. 12, p. 185, 1948.
2. WILSHAW, T. R., RAU, C. A. and TETELMAN, A. S. 'A general model to predict the elastic-plastic stress distribution and fracture strength of notched bars in plane strain bending', *Engineering Fracture Mechanics*, vol. 1, p. 191, 1968.
3. KNOTT, J. F. 'Some effects of hydrostatic tension on the fracture behaviour of mild steel', *Journal Iron and Steel Inst.*, vol. 204, p. 104, 1966.
4. OATES, G. 'Effect of hydrostatic stress on cleavage fracture in a mild steel and a low-carbon manganese steel', *Journal Iron and Steel Inst.*, vol. 206, p. 930, 1968.
5. OATES, G. 'The effect of temperature and strain rate on cleavage fracture in a mild steel and a low-carbon manganese steel', to be published.
6. GREEN, A. P. and HUNDY, B. B. 'Initial plastic yielding in notch bend tests', *Journal of the Mechanics and Physics of Solids*, vol. 4, p. 128, 1956.
7. HILL, R. 'The mathematical theory of plasticity', *Oxford University Press*, p. 248 1950.
8. WILSHAW, T. R. and PRATT, P. L. 'On the plastic deformation of Charpy specimens prior to general yield', *Journal of the Mechanics and Physics of Solids*, vol. 14, p. 7, 1966.
9. ALEXANDER, J. M. and KOMOLY, T. J. 'On the yielding of a rigid/plastic bar with an izod notch', *Journal of the Mechanics and Physics of Solids*, vol. 10, p. 265, 1962.
10. OATES, G. and GRIFFITHS, J. R. 'Mechanisms of cleavage fracture initiation in notched and smooth specimens of 3% silicon-iron', to be published.
11. STEIN, D. F. and LOW, J. R. 'Mobility of edge dislocations in silicon-iron crystals', *Journal of Applied Physics*, vol. 31, p. 362, 1960.
12. SMITH, E. 'The nucleation and growth of cleavage microcracks in mild steel', *Prof. Conf. on Physical Basis of Yield and Fracture, Inst. of Physics and Physical Soc., Oxford*, 1966.
13. BROWN, W. F. and SRAWLEY, J. E. 'Plane strain crack toughness testing of high strength metallic materials', *Amer. Soc. for Testing and Materials, S.T.P.*, 410, 1966.
14. OATES, G. 'Influence of fatigue on brittle fracture in mild steel', *Journal Iron and Steel Inst.*, vol. 204, p. 991, 1966.
15. OATES, G. 'The notched fracture behaviour of coarse-grained silicon iron at 77° K, *Acta Met.*, vol. 15, p. 1679, 1967.

16. GRIFFITHS, J. R. and COTTRELL, A. H. 'Notch effects on slip, twinning and fracture in silicon-steel', *Journal of the Mechanics and Physics of Solids*, vol. 15, p. 125, 1967.
17. KNOTT, J. F. 'On stress intensifications in specimens of Charpy geometry prior to general yield', *Journal of the Mechanics and Physics of Solids*, vol. 15, p. 97, 1967.
18. WEIBULL, W. 'A statistical theory of strength of metals', *Proceedings Royal Swedish Institute for Engineering Research*, vol. 193, no. 151, 1939.
19. BIGGS, W. D. 'The brittle fracture of steel', Macdonald and Evans, London, p. 140. 1960.
20. KNOTT, J. F. and COTTRELL, A. H. 'Notch brittleness in mild steel', *Journal Iron and Steel Inst.*, vol. 201, p. 249, 1963.
21. NEUBER, H. 'Theory of notch stresses', *David Taylor Model Basin, U.S. Navy Dept., Translation 74*, 1945.
22. HENDRICKSON, J. A., WOOD, D. S. and CLARK, D. S. 'Prediction of transition temperature in a notched bar impact test', *Trans. A.S.M.*, vol. 51, p. 629, 1959.
23. COTTRELL, A. H. 'Theoretical aspects of radiation damage and brittle fracture in steel pressure vessels', *Iron and Steel Inst. Special Rep. 69*, p. 281, 1961.
24. WELLS, A. A. 'Unstable crack propagation in metals: cleavage and fast fracture', Crack propagation symposium, College of Aeronautics and the Royal Aeronautical Soc., Cranfield, 1961.

Table 1
Analysis of the material

Element	*C*	*Si*	*S*	*P*	*Mn*
Wt. %	0·033	3·09	0·013	0·017	0·07

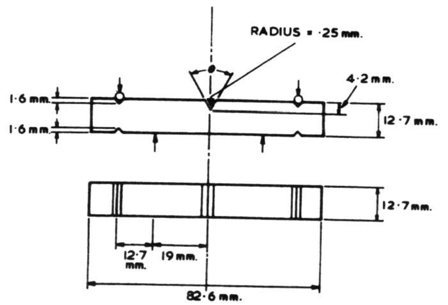

Fig. 1. Design of the notched bond specimen.

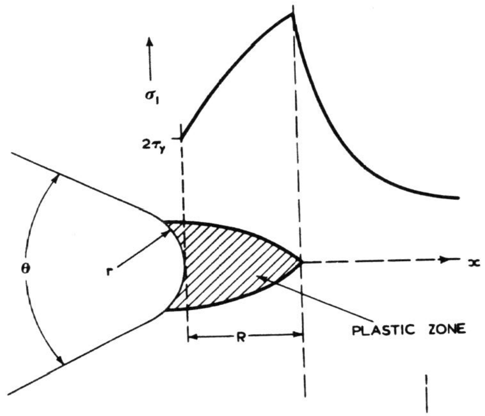

Fig. 2. Schematic longitudinal stress distribution in a notch-bend specimen well below the general yield load.

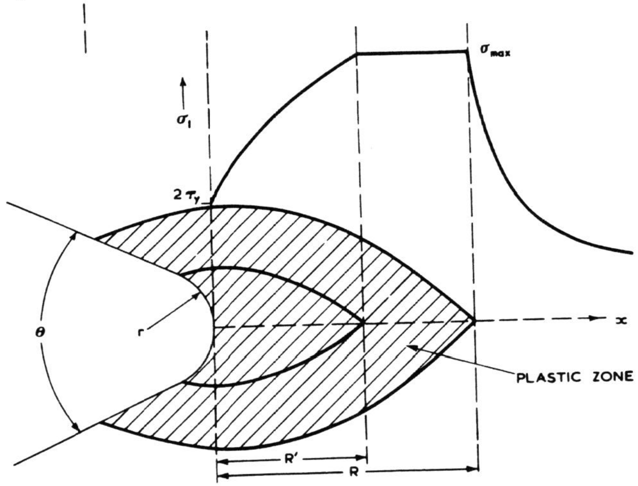

Fig. 3. Schematic longitudinal stress distribution in a notch-bend specimen at general yield.

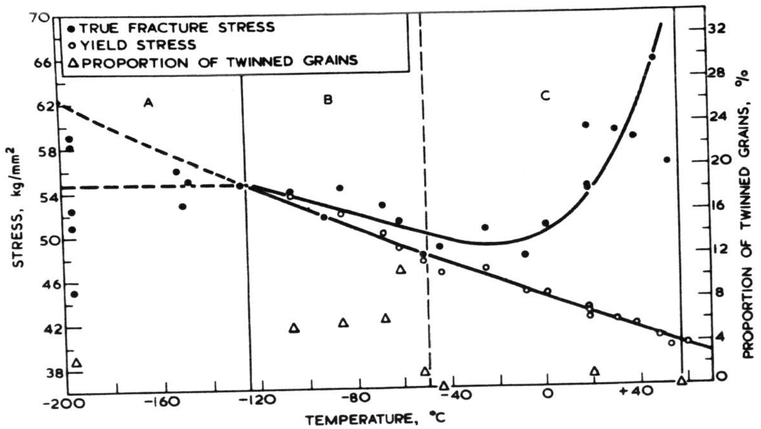

Fig. 4. Yield stress, true fracture stress and incidence of twinning versus temperature for the uniaxial tensile specimens.

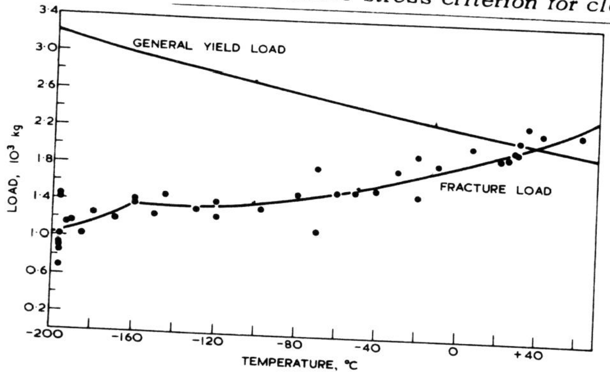

Fig. 5. General yield and fracture loads versus temperature for 45° notch-bend specimens.

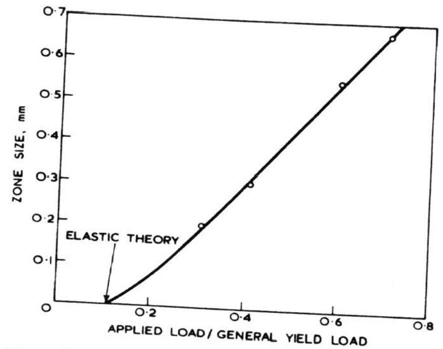

Fig. 6. Extent of plasticity beneath a notch as a function of applied load.

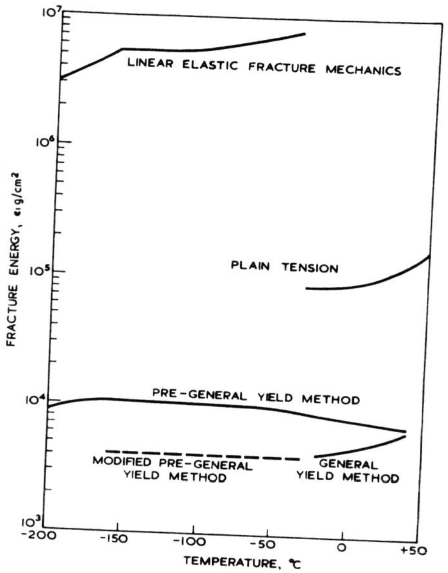

Fig. 8. Calculations of γ using various techniques.

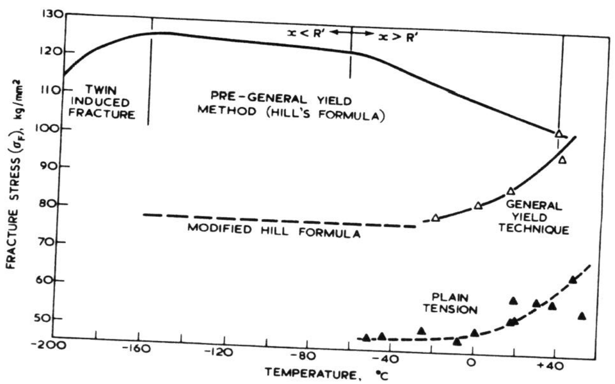

Fig. 7. Fracture stresses of smooth specimens, and calculated σ_F values for the various notch-bend specimens, versus temperature.